KFA

KERNFORSCHUNGSANLAGE JÜLICH GmbH

Institut für Reaktorbauelemente

Flow and Heat Transfer in Packed Beds at low Reynolds Numbers

by

T. Takizuka

Jül - 1739
September 1981
ISSN 0366-0885

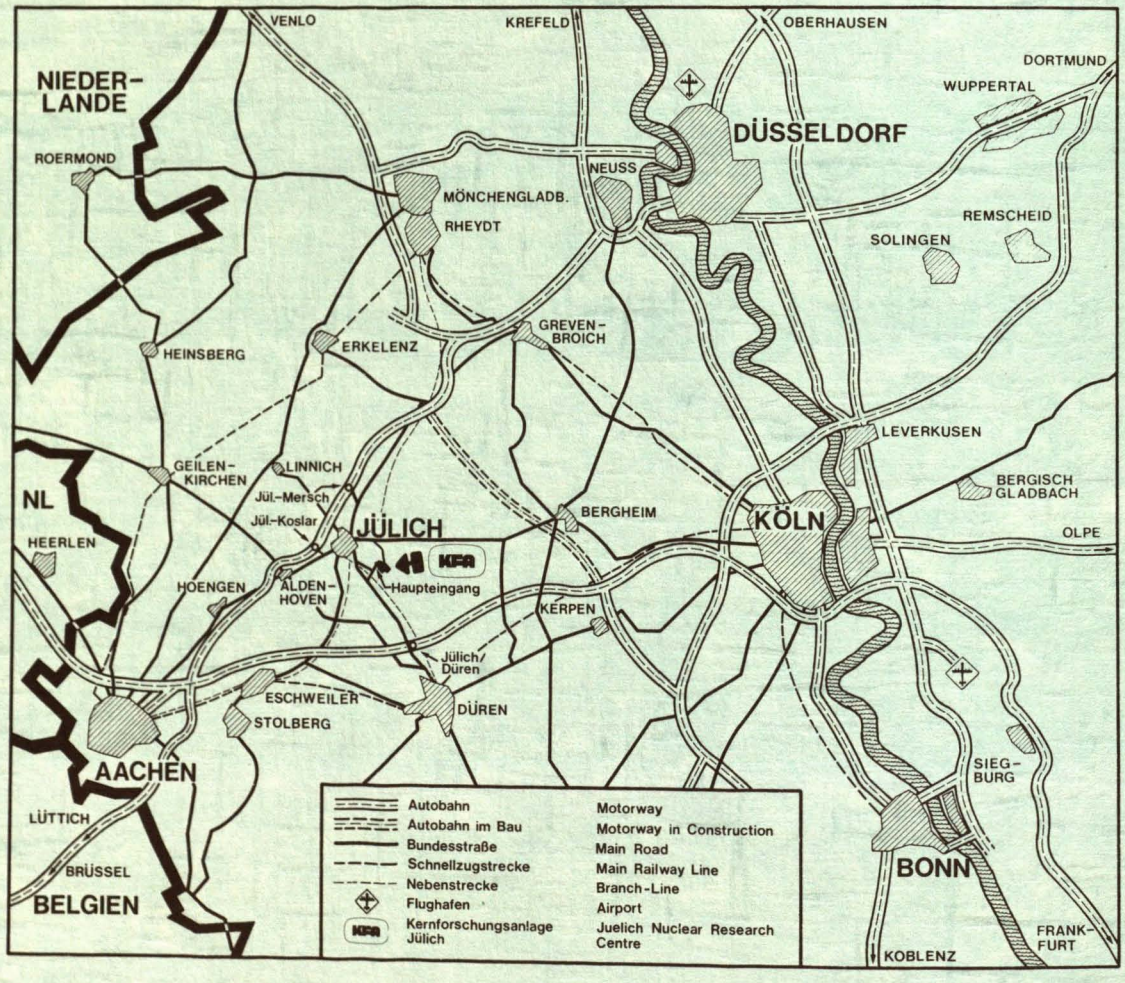

Als Manuskript gedruckt

Berichte der Kernforschungsanlage Jülich – Nr. 1739

Institut für Reaktorbauelemente Jül - 1739

Zu beziehen durch: ZENTRALBIBLIOTHEK der Kernforschungsanlage Jülich GmbH
Postfach 1913 · D-5170 Jülich (Bundesrepublik Deutschland)
Telefon: 02461/610 · Telex: 833556 kfa d

Flow and Heat Transfer in Packed Beds at low Reynolds Numbers

by

T. Takizuka

Kernforschungs-
anlage Jülich
GmbH IRB

Jül-1739

September 1981

Flow and Heat Transfer in Packed Beds at low Reynolds Numbers

by

Takakazu Takizuka

Abstract

Numerical analyses are described for the flow and heat transfer in packed beds at low Reynolds numbers. An analytical model consists of an infinitely large packed bed of regularly arrayed circular cylinders. Assuming symmetry and periodicity of flow and temperature fields, the coupled Navier-Stokes equations and energy equation were solved numerically using a finite difference approach.

The computational procedure and typical examples of numerical results are presented.

Contents

1. Introduction

The prediction of heat transfer coefficient in the pebble-bed type reactor at low Reynolds numbers is important in course of estimating the maximum fuel temperature at abnormally low flow rate conditions. For the forced convective heat and mass transfer between solid particles and flowing fluids within packed beds, a number of experimental correlations have been reported in the literature. However, the experimental results do not agree well with each other and are some orders of magnitude below the values predicted from theoretical calculation in the region of low Reynolds numbers. This anomalous deterioration of transfer coefficient has received considerable attention regarded as a controversial problem in heat and mass transfer within packed beds, since Kunii and Suzuki /1/ summarized those experimental results from an extensive literature search. For Peclet numbers (Pe = RePr) from about 1oo down to o,o3, the Nusselt and Sherwood number decrease with a slope more than one falling as much as four orders of magnitude below the Ranz equation /2/ derived for a single sphere submerged in an infinite media. Many investigators have attempted to explain the behavior of particle-to-fluid heat and mass transfer in packed beds at low Reynolds numbers. The various models have been constructed to show the effective Nusselt or Sherwood number of the overall bed decrease at low Reynolds numbers while the particle-to-fluid Nusselt or Sherwood number (based on local transfer rates and temperature or concentration differences) is suposed to remain constant. The two mechanisms most commonly adopted to the models are nonuniform flow channeling in the bed due to variations in void fraction /1/, /3/, /4/, and diffusion in the flow direction /5/, /6/, /7/. Glicksmaan and Joos /8/ have considered both of these mechanisms together. Another model was formulated by Nelson and Galloway /9/, applying the penetration theory to a particle surrounded by a spherical shell of fluid.

Besides the deterioration in the transfer coefficients, there remains an important problem in heat and mass transfer at low Reynolds numbers. In general, the effect of natural convection on the transfer rates becomes significant as the Reynolds number decreases. To date, only one mass transfer experiment have been done by means of elektrochemical techniques for natural convection and combined forced and natural convection in packed beds /1o/.

Since low Reynolds numbers region is accessible to calculation, a computer program has been developed to give some new results for these problems of

convection in packes beds. An analytical model consists of an infinitely large packed bed of regularly arrayed circular cylinders. Assuming symmetry and periodicity of flow and temperature fields, the coupled Navier-Stokes equations and energy equation were solved numerically using a finite difference approach.

For brevity, the treatment is given here for in-line array only. The numerical scheme developed here can be modified without difficulty for application to staggered array and other arrays with regular geometries.

2. Analysis

2.1 Analytical Model

In the following we shall introduce a simple model to handle the particle-to-fluid heat transfer in packed beds. The model for packed bed consists of an in-line array of circular cylinders extending infinitely in all three dimensions. The pitches of the array is the same both in the mean flow direction and in the lateral direction. All the cylinders have the same diameters. This regular arrangement of the model imposes a high degree of symmetry and periodicity on the problem when the flow field is fully developed, so that the flow need only be solved for one unit cell within the bed. In the case of the temperature field, fully developed situation is attained by applying a constant temperature rise across the cell. The solution domain is shown in figure 1. The void fraction is related with the pitch d and the cylinder radius r_a as $\varepsilon = 1 - \pi (r_a/d)^2$. The mean flow direction is upward and the gravity vector is taken to be in a downward vertical direction. Aiding flow condition is established for the positive value of gravitational acceleration or Grashof number, and opposing flow condition for the negative value.

To analyse the flow and heat transfer in the model of packed bed, the following assumptions will now be made:

1) Flow and temperature fields are two-dimensional.
2) Bousinesq approximations are invoked so that fluid density is assumed to be constant except in the bouyancy terms where fluid density is assumed to vary lineraly proportional to the temperature.
3) All other properties of the fluid are constant.

4) The no-slip boundary condition is assumed on the cylinder surface.

5) The effect of viscous dissipation and radiation is negligible.

6) The surface temperature of each cylinder is uniform circumferentially.

2.2 Governing Equations

The unsteady two-dimensional momentum equations of Newtonian fluid flow with constant physical properties other than the density in the buoyancy terms are given in the cylindrical polar coordinates (r, φ) by

$$\rho_o \left(\frac{\partial u}{\partial t} + u\frac{\partial u}{\partial r} + \frac{v}{r}\frac{\partial u}{\partial \varphi} - \frac{v^2}{r}\right) = -\frac{\partial p}{\partial r}$$

$$+ \mu \left(\frac{\partial^2 u}{\partial r^2} + \frac{1}{r}\frac{\partial u}{\partial r} + \frac{1}{r^2}\frac{\partial^2 u}{\partial \varphi^2} - \frac{u}{r^2} - \frac{2}{r^2}\frac{\partial v}{\partial \varphi}\right)$$

$$+ g\beta\rho_o (\theta - \theta_o)\cos\varphi \qquad (1)$$

$$\rho_o \left(\frac{\partial v}{\partial t} + u\frac{\partial v}{\partial r} + \frac{v}{r}\frac{\partial v}{\partial \varphi} + \frac{uv}{r}\right) = -\frac{1}{r}\frac{\partial p}{\partial \varphi}$$

$$+ \mu \left(\frac{\partial^2 v}{\partial r^2} + \frac{1}{r}\frac{\partial v}{\partial r} + \frac{1}{r^2}\frac{\partial^2 v}{\partial \varphi^2} - \frac{v}{r^2} + \frac{2}{r^2}\frac{\partial u}{\partial \varphi}\right)$$

$$- g\beta\rho_o (\theta - \theta_o)\sin\varphi \qquad (2)$$

where u and v are the velocity component in the radial and angular directions, p the pressure, θ the temperature, θ_0 the refference temperature, ρ_0 the density at θ_0, μ the viscosity, g the acceleration due to gravity, β the thermal coefficient of expansion, and t the time. In the momentum equations, the gravity vector was taken to be in a downward vertical direction ($\varphi = \pi$).

The fluid density ρ was assumed to vary with temperature in the buoyancy terms as

$$\rho = \rho_0 [1 + \beta(\theta - \theta_0)] \tag{3}$$

The equation of continuity is

$$\frac{\partial u}{\partial r} + \frac{u}{r} + \frac{1}{r}\frac{\partial v}{\partial \varphi} = 0 \tag{4}$$

For the unsteady two-dimensional temperature field, the energy equation of the flow with constant physical properties is given by

$$\rho_0 c_p \left(\frac{\partial \theta}{\partial t} + u\frac{\partial \theta}{\partial r} + \frac{v}{r}\frac{\partial \theta}{\partial \varphi}\right)$$

$$= \lambda \left(\frac{\partial^2 \theta}{\partial r^2} + \frac{1}{r}\frac{\partial \theta}{\partial r} + \frac{1}{r^2}\frac{\partial^2 \theta}{\partial \varphi^2}\right) \tag{5}$$

where c_p is the specific heat at constant pressure, and λ the thermal conductivity. In the energy equation, the contribution of mean kinematic energy, viscous dissipation and radiation was assumed to be negligible.

The non-dimensional stream function ψ and voricity ζ are defined as

$$\frac{u}{2 r_a w_0} = \frac{1}{r}\frac{\partial \psi}{\partial \varphi}, \qquad \frac{v}{2 r_a w_0} = -\frac{\partial \psi}{\partial r} \tag{6}$$

$$\zeta = -\frac{2r_a}{w_o}\left(\frac{\partial v}{\partial r} + \frac{v}{r} - \frac{1}{r}\frac{\partial u}{\partial \varphi}\right) \tag{7}$$

where r_a is the radius of the cylinder and w_o the superficial velocity of the flow through the bed. It is noted that the equation of continuity (4) is automatically satisfied by introducing the stream function.

Transforming the independent variable r by

$$\xi = \log\left(\frac{r}{2r_a}\right) \tag{8}$$

momentum equations (1) and (2) can be written in the dimensionless form

$$\frac{\partial \zeta}{\partial T} + \frac{1}{h^2}\left(\frac{\partial \psi}{\partial \varphi}\frac{\partial \zeta}{\partial \xi} - \frac{\partial \psi}{\partial \xi}\frac{\partial \zeta}{\partial \varphi}\right)$$

$$= \frac{1}{Re}\frac{1}{h^2}\left(\frac{\partial^2 \zeta}{\partial \xi^2} + \frac{\partial^2 \zeta}{\partial \varphi^2}\right)$$

$$- \frac{Gr}{Re^2}\frac{1}{h}\left(\frac{\partial \Theta}{\partial \varphi}\cos\varphi + \frac{\partial \Theta}{\partial \xi}\sin\varphi\right) \tag{9}$$

$$\zeta = -\frac{1}{h^2}\left(\frac{\partial^2 \psi}{\partial \xi^2} + \frac{\partial^2 \psi}{\partial \varphi^2}\right) \tag{10}$$

where Θ is the dimensionless temperature, T the dimensionless time, and h the scale factor. These quantities are nondimensionalized by difining

$$\Theta = \frac{\theta - \theta_o}{\Delta\theta}\,, \qquad T = \frac{w_o}{2r_a}t\,,$$

$$h = \exp(\xi)$$

The characteristic temperature difference $\Delta\theta$ is taken to be equal to the temperature rise of the flow across the solution domain. The Reynolds number Re and the Grashof number Gr in the dimensionless governing equation are based on the cylinder diameter $2r_a$.

$$Re = \frac{2 r_a w_o}{\nu} \tag{11}$$

$$Gr = \frac{g\beta\Delta\theta(2r_a)^3}{\nu^2} \tag{12}$$

where ν is the kinematic viscosity ($\nu = \mu / \rho_o$).

The energy equation (5) can be written similarly in the dimensionless form

$$\frac{\partial \Theta}{\partial t} + \frac{1}{h^2}\left(\frac{\partial \psi}{\partial \varphi}\frac{\partial \Theta}{\partial \xi} - \frac{\partial \psi}{\partial \xi}\frac{\partial \Theta}{\partial \varphi}\right)$$

$$= \frac{1}{Re\,Pr}\frac{1}{h^2}\left(\frac{\partial^2 \Theta}{\partial \xi^2} + \frac{\partial^2 \Theta}{\partial \varphi^2}\right) \tag{13}$$

where Pr is the Prandtl number (Pr = $\mu c_p / \lambda$).

The vorticity transport equation (9) and the energy equation (13) are both parabolic in time, second order, nonlinear, partial differential equations. In contrast to the pure forced convection problem without buoyancy effect, for the present problem, these equations are coupled through the temperature dependent buoyancy term in the vorticity transport equation, so that the flow field can not be solved independently. The stream function equation (1o) is treated as a boundary value problem given by the linear Poisson equation with vorticity as the source function.

2.3 Boundary Conditions

The governing equations are elliptic requiring boundary conditions prescribed around all boundaries of the solution domain. For the problem at hand, four types of boundaries are present, i.e., cylinder surface, center plane, symmetry plane, and inlet and outlet plane, as shown in figure 2.

At the cylinder surface, the two components of the velocity are zero.

$$u = v = 0 \qquad \text{at } r = r_a \tag{14}$$

The surface temperature θ_a is assumed to be circumfentially uniform.

$$\theta = \theta_a \qquad \text{at } r = r_a \tag{15}$$

The value of the surface temperature is determined from the steady state heat balance within the solution domain as

$$-2r_a\lambda \int_0^{\pi} \left.\frac{\partial\theta}{\partial r}\right|_a d\varphi = \rho c_p w_0 d\Delta\theta \tag{16}$$

where d is the pitch of the cylinder array in the bed.

Along the center plane, we have due to symmetry for both the flow and temperature fields

$$v = \frac{\partial u}{\partial \varphi} = 0 \qquad \text{at } \varphi = 0 \text{ and } \pi \tag{17}$$

$$\frac{\partial\theta}{\partial\varphi} = 0 \qquad \text{at } \varphi = 0 \text{ and } \pi \tag{18}$$

On the symmetry plane, the boundary conditions are

$$w_x = \frac{\partial w_y}{\partial x} = 0 \qquad \text{at} \quad x = d/2 \tag{19}$$

$$\frac{\partial \theta}{\partial x} = 0 \qquad \text{at} \quad x = d/2 \tag{20}$$

where w_x and w_y denote the velocity components in the x and y directions.

In the present study attention is limited to the region where both the flow and temperature field are fully developed in a packed bed of regularly arrayed circular cylinders. The flow pattern is exactly repeated from one row to the next in this situation. For this periodic flow pattern, the values of the velocity components w_x and w_y are the same on the inlet plane ($y = -d/2$) as on the outlet plane ($y = d/2$).

$$\begin{aligned} w_x(x, d/2) &= w_x(x, -d/2) \\ w_y(x, d/2) &= w_y(x, -d/2) \end{aligned} \tag{21}$$

In the case of the temperature, taking the temperature rise due to the heat transferred from the cylinder into account we have

$$\theta(x, d/2) = \theta(x, d/2) + \Delta\theta \tag{22}$$

By using the non-dimensional variables introduced in the previous section, the boundary conditions above now read as follows.

Cylinder Surface (at $R = R_a$). Around the stational cylinder with an inpermeable wall, the value of the stream function is constant and is set to zero. The gradient of the stream function normal to the surface is zero.

$$\Psi = \frac{\partial \Psi}{\partial \xi} = 0 \tag{23}$$

$$\Theta = \Theta_a \tag{24}$$

The dimensionless surface temperature Θ_a is calculated by

$$-2\int_0^{\pi} \left.\frac{\partial \Theta}{\partial \xi}\right|_a d\varphi = RePrD \tag{25}$$

where D is the dimensionless pitch of the array ($D = d/(2r_a)$).

Center Plane (at $\varphi = 0$ and π). The value of the stream function on the center plane is zero. The vorticity and the gradient of the dimensionless temperature normal to the center plane are both zero.

$$\psi = \zeta = 0 \tag{26}$$

$$\frac{\partial \Theta}{\partial \varphi} = 0 \tag{27}$$

Symmetry Plane (at X = D/2). On the symmetry plane the stream function is set to a constant value ψ_s. This value corresponds to the dimensionless flow rate through the solution domain. The vorticity and the gradient of the dimensionless temperature normal to the symmetry plane are both zero.

$$\psi = \psi_s \quad \left(= \frac{D}{4Ra}\right)$$

$$\zeta = 0 \tag{28}$$

$$\frac{\partial \Theta}{\partial X} = 0 \tag{29}$$

where $X = x/(2r_a)$.

Inlet and Outlet Plane (at Y = - D/2 and D/2). The values of the stream function and the vorticity on the outlet plane are the same as those on the inlet plane.

$$\Psi(X, D/2) = \Psi(X, -D/2)$$

$$\zeta(X, D/2) = \zeta(X, -D/2) \tag{3o}$$

The boundary condition for the dimensionless temperature becomes

$$\Theta(X, D/2) = \Theta(X, -D/2) + 1.0 \tag{31}$$

where $Y = y/(2r_a)$.

2.4 Pressure, Friction and Heat Transfer Coefficient

Once the flow field around the cylinder becomes known, the pressure on the cylinder surface can be calculated from the momentum equation (2). On the cylinder surface, equation (2) reduces to

$$\frac{1}{r_a}\frac{\partial P}{\partial \varphi}\bigg|_a = \mu\left(\frac{\partial^2 v}{\partial r^2}\bigg|_a + \frac{1}{r_a}\frac{\partial v}{\partial r}\bigg|_a\right) - g\beta\rho_o(\theta_a - \theta_o)\sin\varphi \tag{32}$$

therefore

$$P_a(\varphi) - P_a(0) = \mu r_a \int_0^{\varphi}\left(\frac{\partial^2 v}{\partial r^2}\bigg|_a + \frac{1}{r_a}\frac{\partial v}{\partial r}\bigg|_a\right) d\varphi$$

$$-g\beta\rho_o(\theta_a - \theta_o) r_a (1 - \cos\varphi) \tag{33}$$

Equation (33) is expressed in non-dimensional form as

$$C_p(\varphi) = \frac{1}{Re}\int_0^{\varphi}\frac{\partial \zeta}{\partial \xi}\bigg|_a d\varphi + \frac{Gr}{Re^2} h_a \Theta_a (\cos\varphi - 1) \tag{34}$$

where C_p is the dimensionless surface pressure or pressure coefficient defined as

$$C_p(\varphi) = \frac{P_a(\varphi) - P_a(0)}{\rho_o w_o^2}$$

The friction stress on the cylinder surface is calculated by

$$\tau(\varphi) = \mu \left.\frac{\partial v}{\partial r}\right|_a \tag{35}$$

The non-dimensional form for equation (35) is

$$C_f(\varphi) = \frac{\zeta_a}{Re} \tag{36}$$

where C_f is the dimensionless friction stress or friction coefficient defined as

$$C_f(\varphi) = \frac{\tau(\varphi)}{\rho_0 w_0^2}$$

The pressure drag coefficient C_{Dp} and the friction drag coefficient C_{Df} are given by the formulae

$$C_{Dp} = -\int_0^{\pi} C_p \cos\varphi \, d\varphi \tag{37}$$

$$C_{Df} = -\int_0^{\pi} C_f \sin\varphi \, d\varphi \tag{38}$$

The total drag coefficient C_D is

$$C_D = C_{Dp} + C_{Df} \tag{39}$$

The local heat transfer coefficient h_1 is defined by

$$h_1(\varphi) = \frac{-\lambda \left.\frac{\partial \theta}{\partial r}\right|_a}{\theta_a - \theta_b} \tag{40}$$

where θ_b is the bulk temperature or mixed mean temperature evaluated on the flow cross section at $\varphi = \pi/2$ as

$$\theta_b = \frac{\int_{r_a}^{d/2} v\theta\big|_{\varphi=\pi/2} dr}{\int_{r_a}^{d/2} v\big|_{\varphi=\pi/2} dr} \tag{41}$$

Equations (4o) and (41) are expressed in non-dimensional form as

$$Nu_l(\varphi) = -\frac{1}{\Theta_a - \Theta_b}\frac{1}{h_a}\frac{\partial \Theta}{\partial \xi}\bigg|_a \tag{42}$$

$$\Theta_b = \frac{1}{\psi_s}\int_{\xi_a}^{\xi_{D/2}} \Theta \frac{\partial \psi}{\partial \xi}\bigg|_{\varphi=\pi/2} d\xi \tag{43}$$

where Nu_l is the local Nusselt numer ($Nu_l(\varphi) = 2r_a h_l(\varphi)/\lambda$) and Θ_b the dimensionless bulk temperature ($\Theta_b = (\theta_b - \theta_o)/\Delta\theta$).
Then the mean Nusselt number Nu_m is calculated by averaging the local Nusselt number over the surface of the cylinder.

$$Nu_m = \frac{1}{\pi}\int_0^{\pi} Nu_l \, d\varphi \tag{44}$$

3. Numerical Method

3.1 Finite Difference Approximation

To apply the method of finite difference, the computational domain was divided into a cylindrical polar grid, as shown in figure 3. From equation (8), the radial coordinate in physical plane is expressed as

$$r_i = r_a \exp[(i-1)\Delta\xi]$$

where i denotes the node location in the radial direction, $\Delta\xi$ the grid spacing on the transformed plane. In the angular direction, nodes are uniformly spaced with $\Delta\varphi$, so that

$$\varphi_j = (j-2)\Delta\varphi$$

where j is the angular node location. This grid system lacks coordinate lines coincide with the outer boundaries, i.e., the symmetry plane and the inlet and outlet plane, of the solution domain under study. Therefore the boundary conditions on the outer boundaries are implemented by introducing external nodes and false nodes to the grid as described later.

The governing equations are solved by using finite difference method. For the first and second space derivatives, the equations were approximated by the central difference scheme. The central difference scheme is usually recommended because of its high accuracy and efficiency in comparison with the upwind difference scheme or other finite difference schemes applicable to elliptic-type convection equations. For the time derivatives, implicit scheme was adopted. In finite difference methods for solving parabolic partial differential equations, implicit scheme is generally used to avoid severe restrictions on the time increment. In the implicit scheme, the equations are solved iteratively by Crank-Nikolson method.

Dimensionless vorticity transport equation (9) becomes

$$\begin{aligned}
{}^{n+1}\zeta_{i,j}^{T+\Delta T} = \zeta_{i,j}^{T} + \frac{\Delta T}{2}\Bigg[& -\frac{1}{h_i^2}\left(\frac{\psi_{i,j+1}^{T}-\psi_{i,j-1}^{T}}{2\Delta\varphi}\,\frac{\zeta_{i+1,j}^{T}-\zeta_{i-1,j}^{T}}{2\Delta\xi}\right. \\
& \left. -\frac{\psi_{i+1,j}^{T}-\psi_{i-1,j}^{T}}{2\Delta\xi}\,\frac{\zeta_{i,j+1}^{T}-\zeta_{i,j-1}^{T}}{2\Delta\varphi}\right) \\
& +\frac{1}{Re}\,\frac{1}{h_i^2}\left(\frac{\zeta_{i+1,j}^{T}-2\zeta_{i,j}^{T}+\zeta_{i-1,j}^{T}}{\Delta\xi^2}+\frac{\zeta_{i,j+1}^{T}-2\zeta_{i,j}^{T}+\zeta_{i,j-1}^{T}}{\Delta\varphi^2}\right)
\end{aligned}$$

$$-\frac{Gr}{Re^2}\frac{1}{h_i}\left(\frac{\Theta^{T}_{i,j+1}-\Theta^{T}_{i,j-1}}{2\Delta\varphi}\cos\varphi_j+\frac{\Theta^{T}_{i+1,j}-\Theta^{T}_{i-1,j}}{2\Delta\xi}\sin\varphi_j\right)$$

$$-\frac{1}{h_i^2}\left(\frac{{}^{n}\psi^{T+\Delta T}_{i,j+1}-{}^{n}\psi^{T+\Delta T}_{i,j-1}}{2\Delta\varphi}\,\frac{{}^{n}\zeta^{T+\Delta T}_{i+1,j}-{}^{n}\zeta^{T+\Delta T}_{i-1,j}}{2\Delta\xi}\right.$$

$$\left.-\frac{{}^{n}\psi^{T+\Delta T}_{i+1,j}-{}^{n}\psi^{T+\Delta T}_{i-1,j}}{2\Delta\xi}\,\frac{{}^{n}\zeta^{T+\Delta T}_{i,j+1}-{}^{n}\zeta^{T+\Delta T}_{i,j-1}}{2\Delta\varphi}\right)$$

$$+\frac{1}{Re}\frac{1}{h_i^2}\left(\frac{{}^{n}\zeta^{T+\Delta T}_{i+1,j}-2\,{}^{n}\zeta^{T+\Delta T}_{i,j}+{}^{n}\zeta^{T+\Delta T}_{i-1,j}}{\Delta\xi^2}+\frac{{}^{n}\zeta^{T+\Delta T}_{i,j+1}-2\,{}^{n}\zeta^{T+\Delta T}_{i,j}+{}^{n}\zeta^{T+\Delta T}_{i,j-1}}{\Delta\varphi^2}\right)$$

$$\left.-\frac{Gr}{Re^2}\frac{1}{h_i}\left(\frac{{}^{n}\Theta^{T+\Delta T}_{i,j+1}-{}^{n}\Theta^{T+\Delta T}_{i,j-1}}{2\Delta\varphi}\cos\varphi_j+\frac{{}^{n}\Theta^{T+\Delta T}_{i+1,j}-{}^{n}\Theta^{T+\Delta T}_{i-1,j}}{2\Delta\xi}\sin\varphi_j\right)\right] \tag{45}$$

where $\zeta^{T}_{i,j}$, $\psi^{T}_{i,j}$ and $\Theta^{T}_{i,j}$ denote the vorticity, stream function and temperature respectively at the node (i, j) at the time T. Since this finite difference equation contains the unknown variables at the time T + ΔT in both sides, iterative computation for the vorticity together with the stream function and temperature is required until convergence is achieved. The number of the iteration is represented by n. Procedure of iteration and convergence criteria are described in the following section.

From equation (1o), finite difference representation for the stream function is given by

$$\psi_{i,j}=\frac{1}{2(\Delta\xi^2+\Delta\varphi^2)}\left[(\psi_{i+1,j}+\psi_{i-1,j})\Delta\varphi^2+(\psi_{i,j+1}\right.$$

$$+ \psi_{i,j-1})\Delta\xi^2 + h_i^2 \zeta_{i,j} \Delta\xi^2 \Delta\varphi^2 \Big] \tag{46}$$

The energy equation (13) becomes

$$\begin{aligned}
{}^{n+1}\Theta_{i,j}^{T+\Delta T} = \Theta_{i,j}^{T} + \frac{\Delta T}{2}\Bigg[& -\frac{1}{h_i^2}\left(\frac{\psi_{i,j+1}^{T} - \psi_{i,j-1}^{T}}{2\Delta\varphi}\,\frac{\Theta_{i+1,j}^{T} - \Theta_{i-1,j}^{T}}{2\Delta\xi}\right. \\
& \left. - \frac{\psi_{i+1,j}^{T} - \psi_{i-1,j}^{T}}{2\Delta\xi}\,\frac{\Theta_{i,j+1}^{T} - \Theta_{i,j-1}^{T}}{2\Delta\varphi}\right) \\
& + \frac{1}{RePr}\,\frac{1}{h_i^2}\left(\frac{\Theta_{i+1,j}^{T} - 2\Theta_{i,j}^{T} + \Theta_{i-1,j}^{T}}{\Delta\xi^2} + \frac{\Theta_{i,j+1}^{T} - 2\Theta_{i,j}^{T} + \Theta_{i,j-1}^{T}}{\Delta\varphi^2}\right) \\
& - \frac{1}{h_i^2}\left(\frac{{}^{n}\psi_{i,j+1}^{T+\Delta T} - {}^{n}\psi_{i,j-1}^{T+\Delta T}}{2\Delta\varphi}\,\frac{{}^{n}\Theta_{i+1,j}^{T+\Delta T} - {}^{n}\Theta_{i-1,j}^{T+\Delta T}}{2\Delta\xi}\right. \\
& \left. - \frac{{}^{n}\psi_{i+1,j}^{T+\Delta T} - {}^{n}\psi_{i-1,j}^{T+\Delta T}}{2\Delta\xi}\,\frac{{}^{n}\Theta_{i,j+1}^{T+\Delta T} - {}^{n}\Theta_{i,j-1}^{T+\Delta T}}{2\Delta\varphi}\right) \\
& + \frac{1}{RePr}\,\frac{1}{h_i^2}\left(\frac{{}^{n}\Theta_{i+1,j}^{T+\Delta T} - 2\,{}^{n}\Theta_{i,j}^{T+\Delta T} + {}^{n}\Theta_{i-1,j}^{T+\Delta T}}{\Delta\xi^2} - \frac{{}^{n}\Theta_{i,j+1}^{T+\Delta T} - 2\,{}^{n}\Theta_{i,j}^{T+\Delta T} + {}^{n}\Theta_{i,j-1}^{T+\Delta T}}{\Delta\varphi^2}\right)\Bigg]
\end{aligned} \tag{47}$$

The boundary conditions are presented in the form of finite difference as follows.

On the cylinder surface at $R = R_a$ ($i = 1$), the value of the stream function is zero.

$$\psi_{1,j} = 0 \tag{48}$$

The boundary value of the vorticity can not be evaluated directly, since it depends on the velocity gradients at the surface. The Taylor expansions of the stream function and vorticity on the surface are

$$\psi_{2,j} = \psi_{1,j} + \left.\frac{\partial\psi}{\partial\xi}\right|_{1,j}\Delta\xi + \frac{1}{2!}\left.\frac{\partial^2\psi}{\partial\xi^2}\right|_{1,j}\Delta\xi^2 + \frac{1}{3!}\left.\frac{\partial^3\psi}{\partial\xi^3}\right|_{1,j}\Delta\xi^3 + \cdots\cdots \tag{49}$$

$$\zeta_{2,j} = \zeta_{1,j} + \left.\frac{\partial\zeta}{\partial\xi}\right|_{1,j}\Delta\xi + \cdots\cdots \tag{5o}$$

For the stream function on the surface we have following relations.

$$\left.\frac{\partial\psi}{\partial\xi}\right|_{1,j} = 0$$

$$\left.\frac{\partial^2\psi}{\partial\xi^2}\right|_{1,j} = -h_1^2\,\zeta_{1,j}$$

$$\left.\frac{\partial^3\psi}{\partial\xi^3}\right|_{1,j} = -h_1^2\left.\frac{\partial\zeta}{\partial\xi}\right|_{1,j}$$

From these relations and equations (48) - (5o), we obtain for the vorticity at the cylinder surface

$$\zeta_{1,j} = -\frac{3\psi_{2,j}}{h_1^2\,\Delta\xi^2} - \frac{\zeta_{2,j}}{2} \tag{51}$$

The surface temperature Θ_1 is evaluated from the boundary condition (25). Approximating the integral around the cylinder by using Simpson's rule for numerical integration

$$\int_0^{\pi} \left.\frac{\partial \Theta}{\partial \xi}\right|_{R=Ra} d\varphi = \frac{\Delta\varphi}{2} \sum_{j=2}^{jmax+1} \left(\left.\frac{\partial \Theta}{\partial \xi}\right|_{1,j} + \left.\frac{\partial \Theta}{\partial \xi}\right|_{1,j+1} \right)$$

and the gradients of the temperature normal to the surface by following numerical differentiation

$$\left.\frac{\partial \Theta}{\partial \xi}\right|_{1,j} = \frac{-3\Theta_1 + 4\Theta_{2,j} - \Theta_{3,j}}{2\Delta\xi}$$

we obtain for the temperature at the cylinder surface

$$\Theta_1 = \frac{RePrD\Delta\xi}{3\pi} - \frac{\Delta\varphi}{6\pi} \sum_{j=2}^{jmax+1} (4\Theta_{2,j} - \Theta_{3,j} + 4\Theta_{2,j+1} - \Theta_{3,j+1}) \tag{52}$$

On the center plane at $\varphi = 0$ and π (j = 2 and jmax + 2), the stream function and vorticity are both set to zero.

$$\psi_{i,2} = \psi_{i,jmax+2} = 0 \tag{53}$$

$$\zeta_{i,2} = \zeta_{i,jmax+2} = 0 \tag{54}$$

The gradients of the temperature normal to the center plane are zero, hence

$$\Theta_{i,1} = \Theta_{i,3}$$

$$\Theta_{i,jmax+3} = \Theta_{i,jmax+1} \tag{55}$$

The condition at the outer boundaries, i.e., the symmetry plane and the inlet and outlet plane, are not so easily handled owing to the lack of coordinate lines coincide with these boundaries. External nodes and false nodes were introduced to the grid in the outer boundary region as shown in figure 4. The external nodes are located at the node points of original grid extended just outside the boundary and false nodes are positioned within the solution domain symmetrically along the boundary to the external nodes. The boundary

conditions provide the relation between the values of the dependent variables at the external nodes and those at the false nodes. The values of the dependent variables at the false nodes are obtained by interpolation from the values at four surrownding nodes. Reffering to the notation in figure 5, the interpolation gives the value of any dependent variable γ at the false node (r_c, φ_c) as

$$\gamma_c = \frac{1}{(r_{i+1} - r_i)(\varphi_{j+1} - \varphi_j)} \left[\gamma_{i,j} (r_{i+1} - r_c)(\varphi_{j+1} - \varphi_c) \right.$$

$$+ \gamma_{i+1,j} (r_c - r_i)(\varphi_{j+1} - \varphi_c) + \gamma_{i,j+1} (r_{i+1} - r_c)(\varphi_c - \varphi_j)$$

$$\left. + \gamma_{i+1,j+1} (r_c - r_i)(\varphi_c - \varphi_j) \right] \qquad (56)$$

The values of the stream function, vorticity and temperature at the external nodes in the region of symmetry boundary are related to the values at the corresponding false nodes from the boundary conditions (28) and (29) by

$$\Psi_{es} = 2\Psi_s - \Psi_{cs} \qquad (57)$$

$$\zeta_{es} = -\zeta_{cs} \qquad (58)$$

$$\Theta_{es} = \Theta_{cs} \qquad (59)$$

where subscripts es and cs denote the values at the external nodes and those at the false nodes in the symmetry boundary region, respctively. As showhn in figure 6(a), the relation of the coordinates between the external node (x_{es}, y_{es}) and the corresponding false node (x_{cs}, y_{cs}) are

$$x_{cs} = d - x_{es} \quad , \qquad y_{cs} = y_{es}$$

From the boundary condition (3o) for the inlet and outlet plane, the values of the stream function and vorticity are the same at the upstream and downstream external nodes as at the corresponding false nodes in the regions of downstream and upstream boundaries respctively.

$$\psi_{eu} = \psi_{cd} \tag{60}$$

$$\zeta_{eu} = \zeta_{cd} \tag{61}$$

$$\psi_{ed} = \psi_{cu} \tag{62}$$

$$\zeta_{ed} = \zeta_{cu} \tag{63}$$

where subscripts eu and ed denote the values at the upstream and downstream external nodes, cu and cd the values at the upstream and downstream false nodes. As shown in figure 6 (b) and 6 (c), the coordinates of these nodes are related by

$$x_{cd} = x_{eu}\ , \qquad y_{cd} = d + y_{eu}$$

$$x_{cu} = x_{ed}\ , \qquad y_{cu} = -d + y_{ed}$$

Similarly, boundary condition (31) for the temperature at the inlet and outlet plane is expressed as

$$\Theta_{eu} = \Theta_{cd} - 1 \tag{64}$$

$$\Theta_{ed} = \Theta_{cu} + 1 \tag{65}$$

The pressure coefficient C_p at the surface is calculated from equation (34). Approximating the integral around the cylinder by

$$\int_0^{\varphi} \left.\frac{\partial \zeta}{\partial \xi}\right|_{R=R_a} d\varphi = \frac{\Delta\varphi}{2} \sum_{j=3}^{j} \left(\left.\frac{\partial \zeta}{\partial \xi}\right|_{1,j-1} + \left.\frac{\partial \zeta}{\partial \xi}\right|_{1,j} \right)$$

and the gradients of the vorticity normal to the surface by

$$\left.\frac{\partial \zeta}{\partial \xi}\right|_{1,j} = \frac{-3\zeta_{1,j} + 4\zeta_{2,j} - \zeta_{3,j}}{2\Delta\xi}$$

we obtain for the pressure at the cylinder surface

$$C_{P_j} = \frac{1}{4Re}\frac{\Delta\varphi}{\Delta\xi}\sum_{j=3}^{j}(-3\zeta_{1,j-1} + 4\zeta_{2,j-1} - \zeta_{3,j-1}$$

$$- 3\zeta_{1,j} + 4\zeta_{2,j} - \zeta_{3,j})$$

$$+ \frac{Gr}{Re^2} h_1 \Theta_1 (\cos\varphi_j - 1) \tag{66}$$

From equation (36), the friction coefficient C_f becomes

$$C_{f_j} = \frac{\zeta_{1,j}}{Re} \tag{67}$$

The pressure drag coefficient C_{Dp} and friction drag coefficient C_{Df} are

$$C_{D_p} = \frac{\Delta\varphi}{2}\sum_{j=2}^{jmax+1}(-C_{P_j}\cos\varphi_j - C_{P_{j+1}}\cos\varphi_{j+1}) \tag{68}$$

$$C_{D_f} = \frac{\Delta\varphi}{2}\sum_{j=2}^{jmax+1}(-C_{f_j}\sin\varphi_j - C_{f_{j+1}}\sin\varphi_{j+1}) \tag{69}$$

From equations (42) and (44), the local Nusselt number Nu_l and mean Nusselt number Nu_m are calculated by the followings.

$$Nu_{l_j} = \frac{-3\Theta_1 + 4\Theta_{2,j} - \Theta_{3,j}}{2\Delta\xi\, h_1 (\Theta_1 - \Theta_b)} \tag{7o}$$

$$Nu_m = \frac{1}{2jmax}\sum_{j=2}^{jmax+1}(Nu_{l_j} + Nu_{l_{j+1}}) \tag{71}$$

3.2 Computational Procedure

The outline of the computational procedure is presented in figure 7.

In the preparation, the spatial coefficients of interpolation for the false nodes are calculated and stored for the following computations of the stream function, vorticity and temperature at outer boundaries. Then, the initial guess for the distributions of stream function and temperature are provided over the entire region of interest. The initial vorticity is calculated from the initial stream function distribution.

The time T is advanced by unit time increment ΔT. Since the boundary conditions do not depend on the time, the unsteady-state problem will converge to the steady-state problem. So in the numerical procedure a convergence iteration technique was applied using the time step as a parameter.

The vorticity field in the solution domain at the time $T + \Delta T$ for the first iteration $n = 1$ is determined from equation (45), in which the values at $T + \Delta T$ for $n = o$ in the right-hand side are taken from the previous time stage. The values of the vorticity at the external nodes are calculated by the boundary conditions (58), (61) and (63) from the values at the false nodes obtained by interpolation.

The stream function is evaluated based on equation (46), using successive - over - relaxation method as

$$ {}^{m+1}\psi_{i,j} = {}^{m}\psi_{i,j} + \omega\left({}^{m+1}\psi_{i,j} - {}^{m}\psi_{i,j}\right) $$

where ω denotes the acceleration parameter and m the iteration parameter for the stream function calculations. This sequence is repeated until the convergence is attained. As convergence criterion we used

$$ \max \left| {}^{m+1}\psi_{i,j} - {}^{m}\psi_{i,j} \right| \leq E_{\psi} $$

where E_{ψ} is the maximum allowable error for the ψ-iteration. The stream functions at the external nodes are calculated by the boundary conditions

(57), (6o) and (62) similarly as in case of the vorticity.

The vorticity at the cylinder surface is given by the boundary condition (51).

Next, the temperature field at T + ΔT is determined from equation (47). The temperatures at the external nodes are calculated by the boundary conditions (59), (64) and (65). The temperature at the cylinder surface is given by the boundary condition (52).

The iteration in the implicit calculations for the vorticity (45) and temperature (47) is terminated when the following two criteria are satisfied together.

$$\max \left| {}^{n+1}\zeta_{i,j} - {}^{n}\zeta_{i,j} \right| \leq E_{u\zeta}$$

$$\max \left| {}^{n+1}\Theta_{i,j} - {}^{n}\Theta_{i,j} \right| \leq E_{u\Theta}$$

Thus, all the values for the vorticity, stream function and temperature are updated. The time is further advanced to the next stage until the vorticity and temperature field do not change in time. As steady state criteria we used

$$\max \left| \zeta_{i,j}^{T+\Delta T} - \zeta_{i,j}^{T} \right| \leq E_{s\zeta}$$

$$\max \left| \Theta_{i,j}^{T+\Delta T} - \Theta_{i,j}^{T} \right| \leq E_{s\Theta}$$

Finally, the steady-state solutions for the vorticity, stream function and temperature are printed out. The results of the fluid dynamic and heat transfer characteristics, such as pressure coefficients, friction coefficients, drag coefficients and Nusselt numbers are obtained from the solution.

4. Results

Flow and temperature fields have been solved for Reynolds number 1o, Grashof number o (pure forced convection), Prandtl number o, and void fraction o.422.

Figure 8 shows the contours of the stream function (streamlines). Flow is separated in the rear portion of the cylinder and is reattached in the front portion of the succeeding cylinder. In this region, the recirculating vortex is formed. The gradients of the stream function in the vortex region are considerably small and the flow is nearly stagnant. On the contrary, the fluied velocity is very high in the side region of the cylinder where the cross section area of the flow is the narrowest. Figure 9 shows the contours of the vorticity. The disributions of the pressure coefficient and friction coefficient along the cylinder surface are presented in figures 1o and 11. In the figure, polar angle φ is measured from the rear stagnation point. The values of drag coefficients are

$$C_{Dp} = 1o7.7$$

$$C_{Df} = 2o.4$$

$$C_{D} = 128.1$$

Figure 12 shows the contours of the temperature. We notice that the greater part of the temperature rise of the flow takes place in the upstream half region of the domain and the thermal equilibrium between the heated cylinder and fluid flow is almost reached in this region. The isothermals close to the front and rear stagnation points are nearly parallel and the temperature varies linearly in the flow direction. Distribution of the local Nusselt number is presented in Figure 13. The maximum heat transfer occurs at $\varphi \doteqdot 125^{o}$, not at the forward stagnation point while the minimum heat transfer takes place at the rear stagnation point. The values of local Nusselt number in the vortex region around the rear stagnation point are negative due to the heat received from the succeeding cylinder with higher surface temperature through conduction in the nealy stagnant fluid. The value of mean Nusselt number is 21.4.

5. Concluding Remarks

The method for using external nodes and false nodes has been successfully applied to the numerical study of the flow and heat transfer characteristics for the simplified model of packed bed. Detail results of the flow and heat transfer characteristics around the cylinder have given by the sample calculation for in-line array at Reynolds number 1o.

Further tasks are the following:

Calculations for the wide range of Reynolds numbers Re, Grashof numbers Gr, Prandtl Numbers Pr and void fractions ε , and establishing the carrelations of the heat transfer characteristics. Adaptation of the method to other two-dimensional array configurations. Extensions of the method to the three-dimensional flow and heat transfer within the regular array of spheres.

Currently work on these tasks is in progress.

Acknowledgement

The autor greatfully acknoledges the helpfull advice and kind support of Dr. E. Achenbach, IRB, KFA Jülich.

Notation

C_D	total drag coefficient
C_{Df}	friction drag coefficient
C_{Dp}	pressure drag coefficient
C_f	friction coefficient
C_p	pressure coefficient
c_p	specific heat at constant pressure
D	nondimensional pitch of the array
d	pitch of the array
E	maximum allowable error in the iteration
g	gravitational acceleration
Gr	Grashof number
h	scale factor
h_l	local heat transfer coefficient
m	iteration parameter for the stream function calculations
n	iteration parameter for the vorticity and temperature calculations in the time
Nu_l	local Nusselt number
Nu_m	mean Nusselt number
p	pressure

Pr	Prandtl number
R	dimensionless radius
r	radial coordinate in the cylindrical polar coordinate system (r, φ)
Re	Reynolds number
T	nondimensional time
t	time
u	velocity component in r-direction
v	velocity component in φ-direction
w_o	superficial velocity
w_x	velocity component in x-direction
w_y	velocity component in y-direction
X, Y	nondimensional cartesian coordinate system
x,y	cartesian coordinate system

Greek symbols

β	volumetric coefficient of thermal expansion
ΔT	nondimensional time increment
$\Delta\theta$	temperature rise across the solution domain
$\Delta\xi$	grid spacing for ξ-coordinate

$\Delta\varphi$ grid spacing for φ-coordinate

ε void fraction

ζ vorticity (nondimensional)

Θ nondimensional temperature

θ temperature

λ thermal conductivity

μ viscosity

ν kinematic viscosity

ξ dimensionless coordinate in the (ξ , φ) coordinate system

ρ density

τ friction stress

φ angular coordinate in the cylindrical polar coordinate system (r, φ)

ψ stream function (nondimensional)

ω acceleration parameter

Subscripts

a cylinder surface

b bulk

c false node

d downstream boundary

e external node

i	space subscript for	ξ -coordinate
j	space subscript for	ψ -coordinate
0	reference condition	
s	symmetry boundary	
u	upstream boundary	

References

/1/ Kunii, D. and Suzuki, M.,
Particle-to-Fluid Heat and Mass Transfer in
Packed Beds of Fine Particles,
Int. J. Heat Mass Transfer, Vol. 1o, pp. 845-852 (1967)

/2/ Ranz, W.E.,
Friction and Transfer Coefficients for Single Particles
and Packed Beds,
Chem. Engng. Progress, Vol. 48, pp. 247-253 (1952)

/3/ Schlünder, E.U.,
On the Mechanism of Mass Transfer in Heterogeneous
Systems - In Particular in Fixed Beds, Fluidized
Beds and on Bubble Trays,
Chem. Engng. Sci., Vol. 32, pp. 845-851 (1977)

/4/ Martin, H.,
Low Peclet Number Particle-to-Fluid Heat and Mass Transfer
in Packed Beds,
Chem. Engng. Sci., Vol. 33, pp. 913-919 (1978)

/5/ Gunn, D.J. and De Souza, J.F.C.,
Heat Transfer and Axial Dispersion in Packed Beds,
Chem. Engng. Sci., Vol. 29, pp. 1363-1371 (1974)

/6/ Sørensen, J.P. and Stewart, W.E.,
Computation of Forced Convection in Slow Flow
through Ducts and Packed Beds - I. Extension of
the Graetz Problem,
Chem. Engng. Sci., Vol. 29, pp. 811-817 (1974)

/7/ Wakao, N. and Funazkri, T.,
Effect of Fluid Dispersion Coefficients on
Particle-to-Fluid Mass Transfer Coefficients
in Packed Beds,
Chem. Engng. Sci., Vol. 33, pp. 1375-1384 (1978)

/8/ Glicksman, L.R. and Joos, F.M.,
Heat and Mass Transfer in Fixed Beds at Low
Reynolds Numbers,
Trans. ASME, J. Heat Transfer, Vol. 1o2, pp. 736-741 (198o)

/9/ Nelson, P.A. and Galloway, T.R.,
Particle-to-Fluid Heat and Mass Transfer in
Dense System of Fine Particles,
Chem. Engng. Sci., Vol. 3o, pp. 1-6 (1975)

/1o/ Karabelas, A.J., Wegner, T.H. and Hanratty, T.J.,
Use of Asymptotic Relations to Correlate Mass Transfer
Data in Packed Beds,
Chem. Engng. Sci., Vol. 26, pp. 1581-1589 (1971)

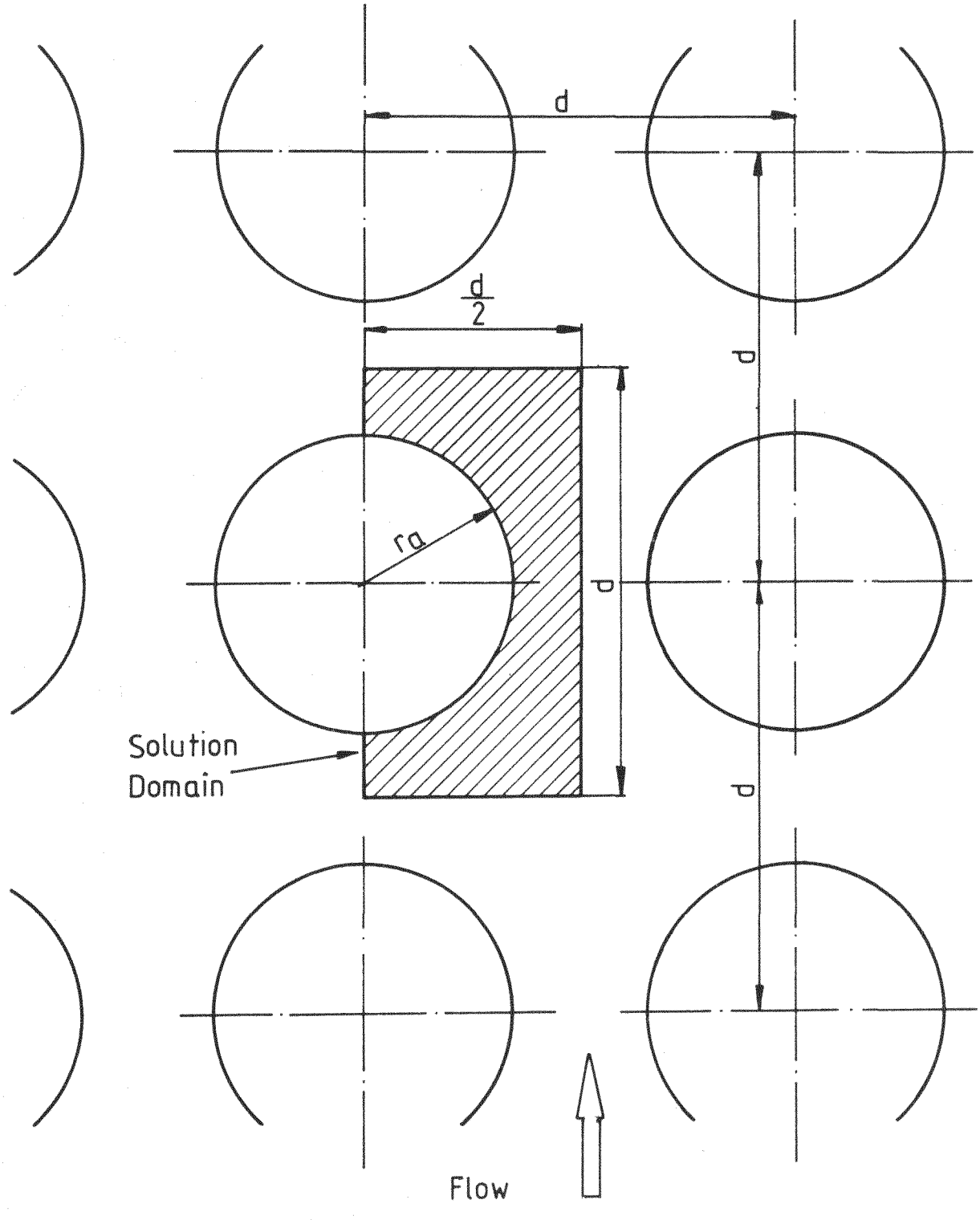

Figure1. Analytical Model of Packed Bed and Solution Domain.

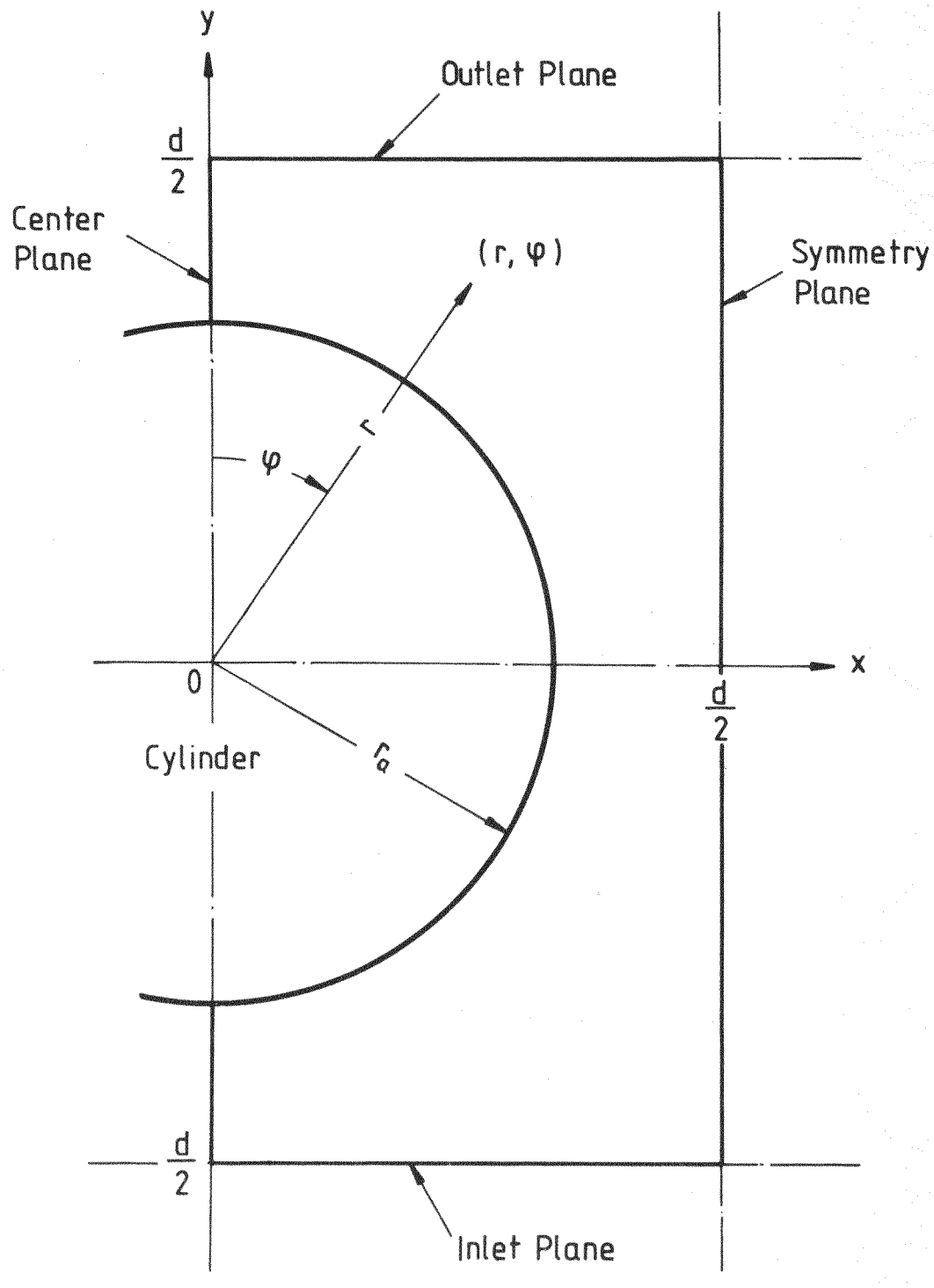

Figure 2 Boundaries of the Solution Domain

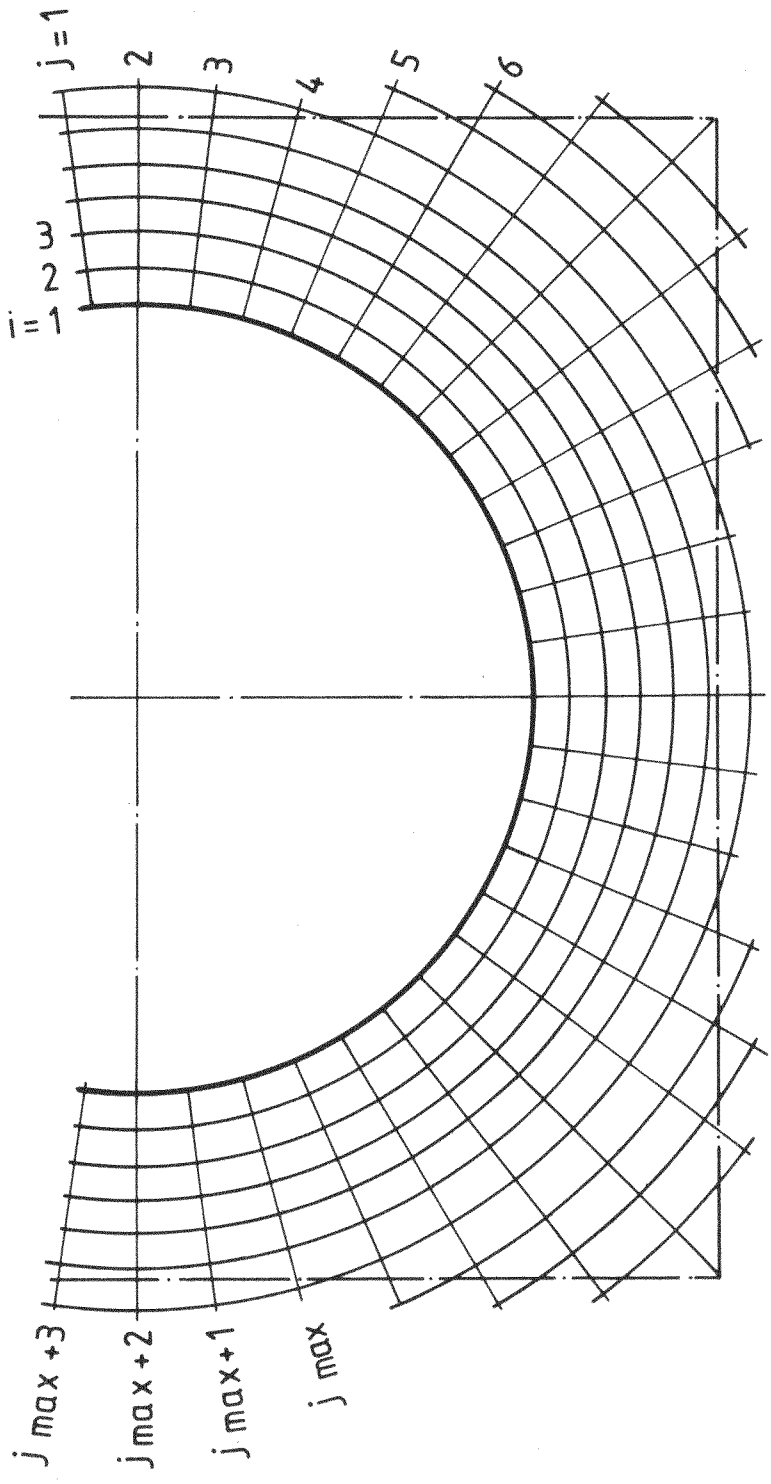

Figure 3. Numerical Grid for Finite-Difference Computation

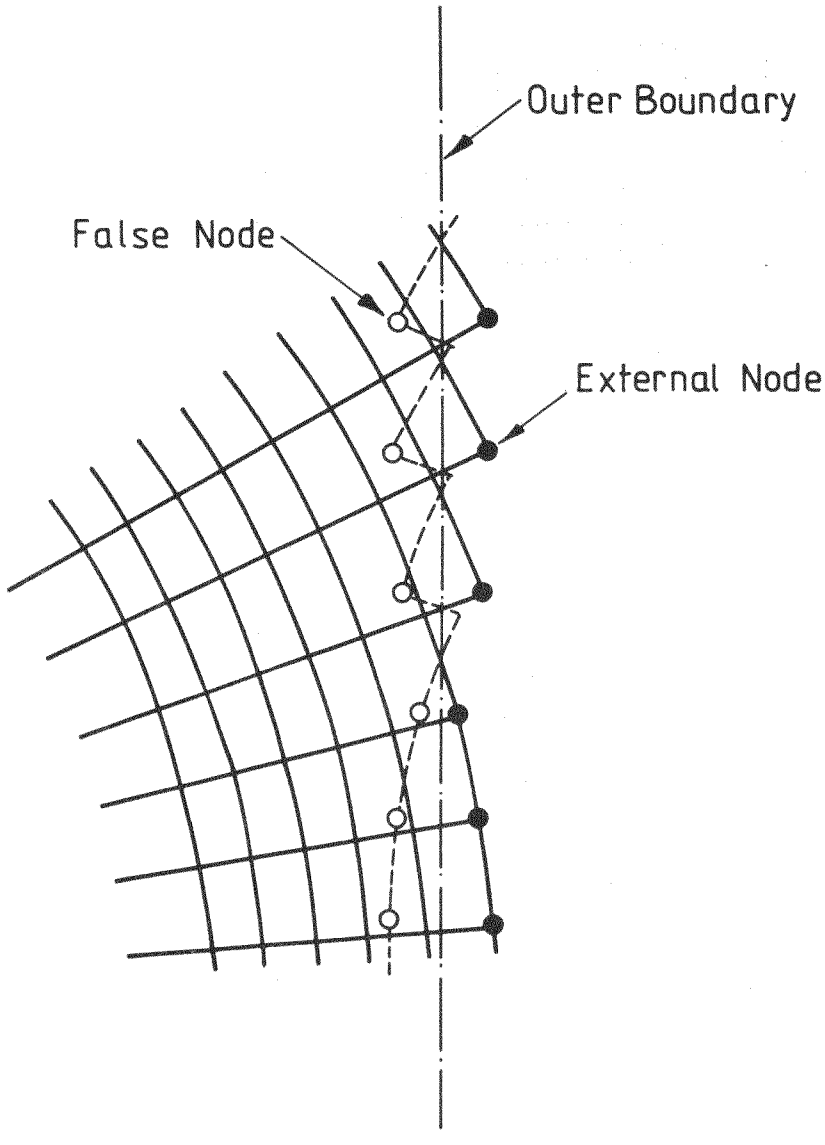

Figure 4. Introduction of External Nodes and False Nodes for Outer Boundary Conditions.

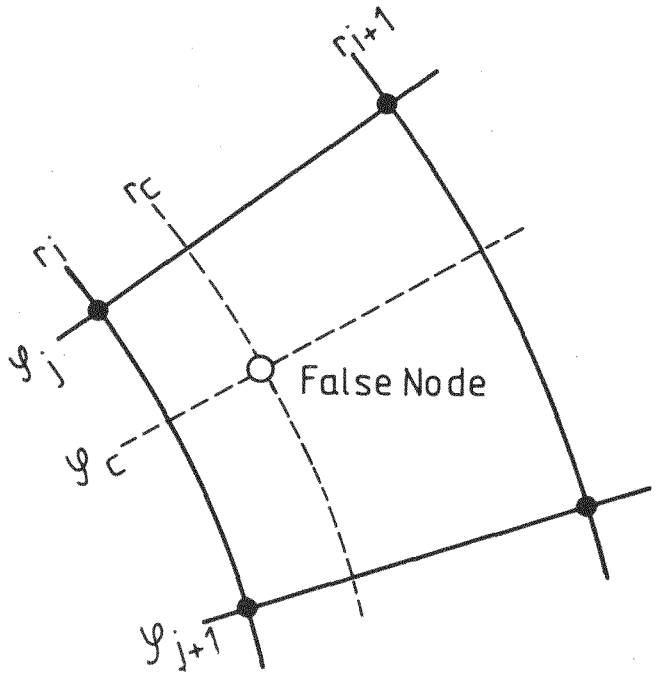

Figure 5. Linear Interpolation Scheme for False Node.

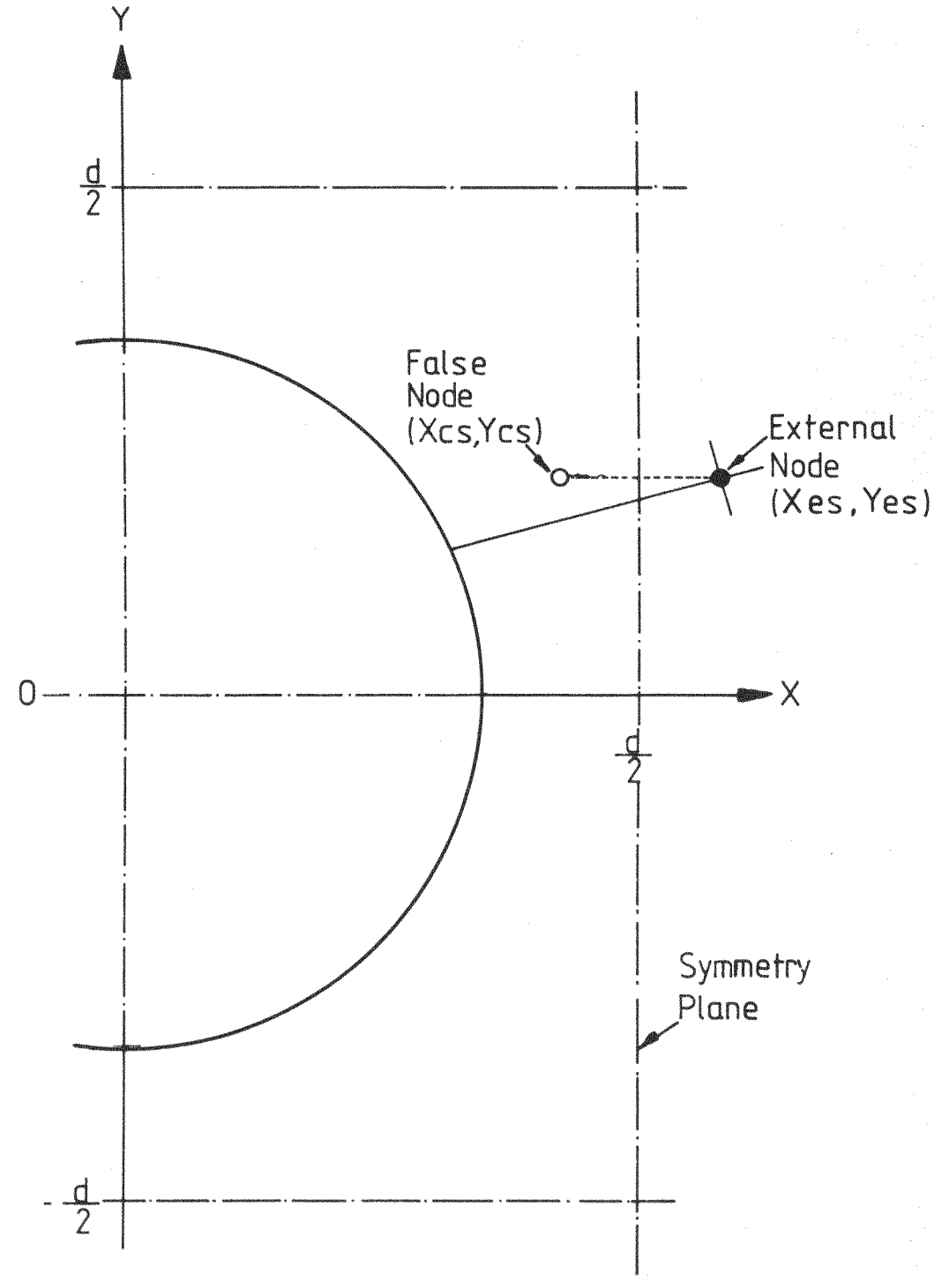

Figure 6(a). External Node and Corresponding False Node for the Symmetry Boundary.

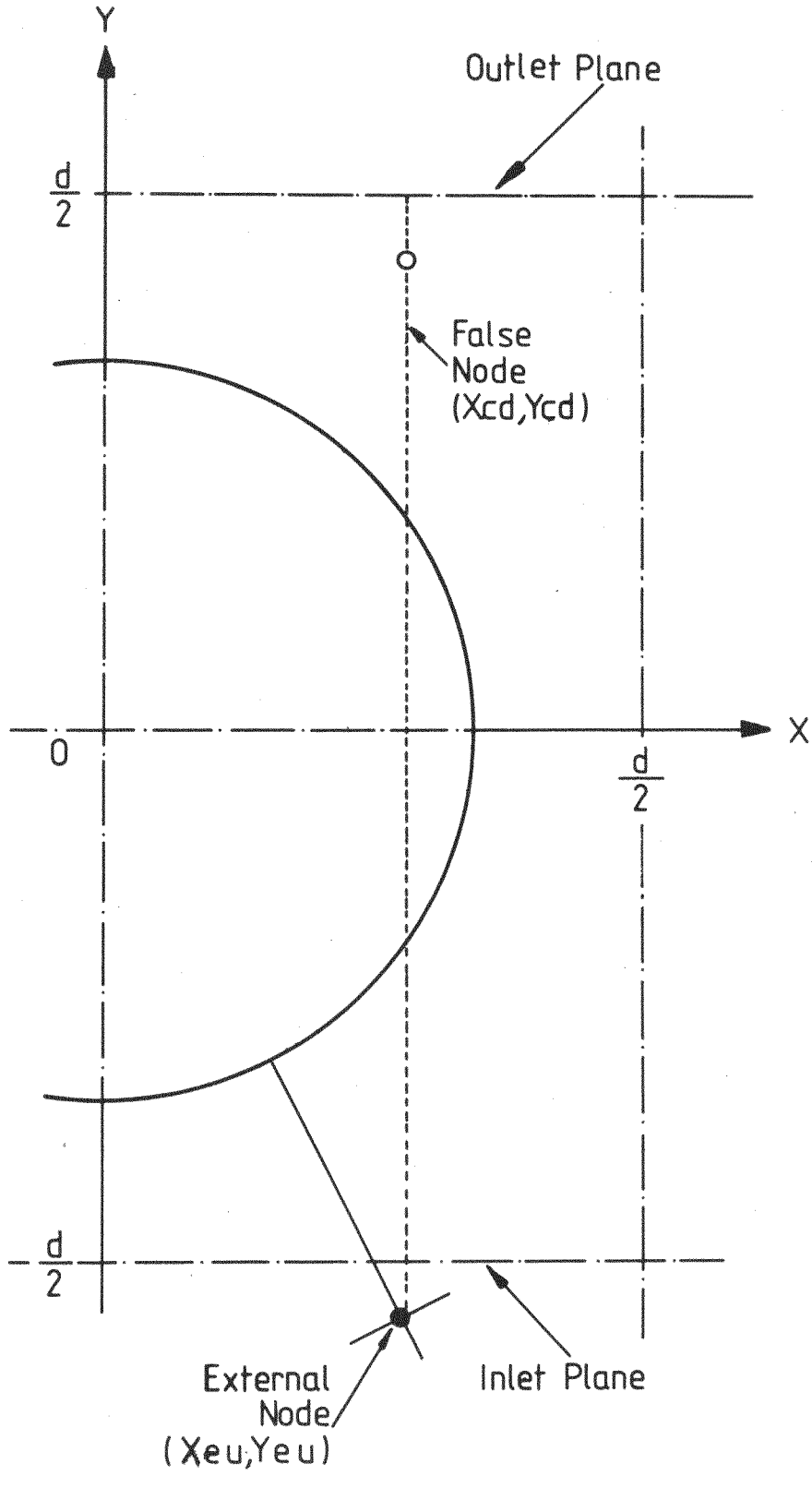

Figure 6(b) Upstream External Node and Corresponding Downstream False Node.

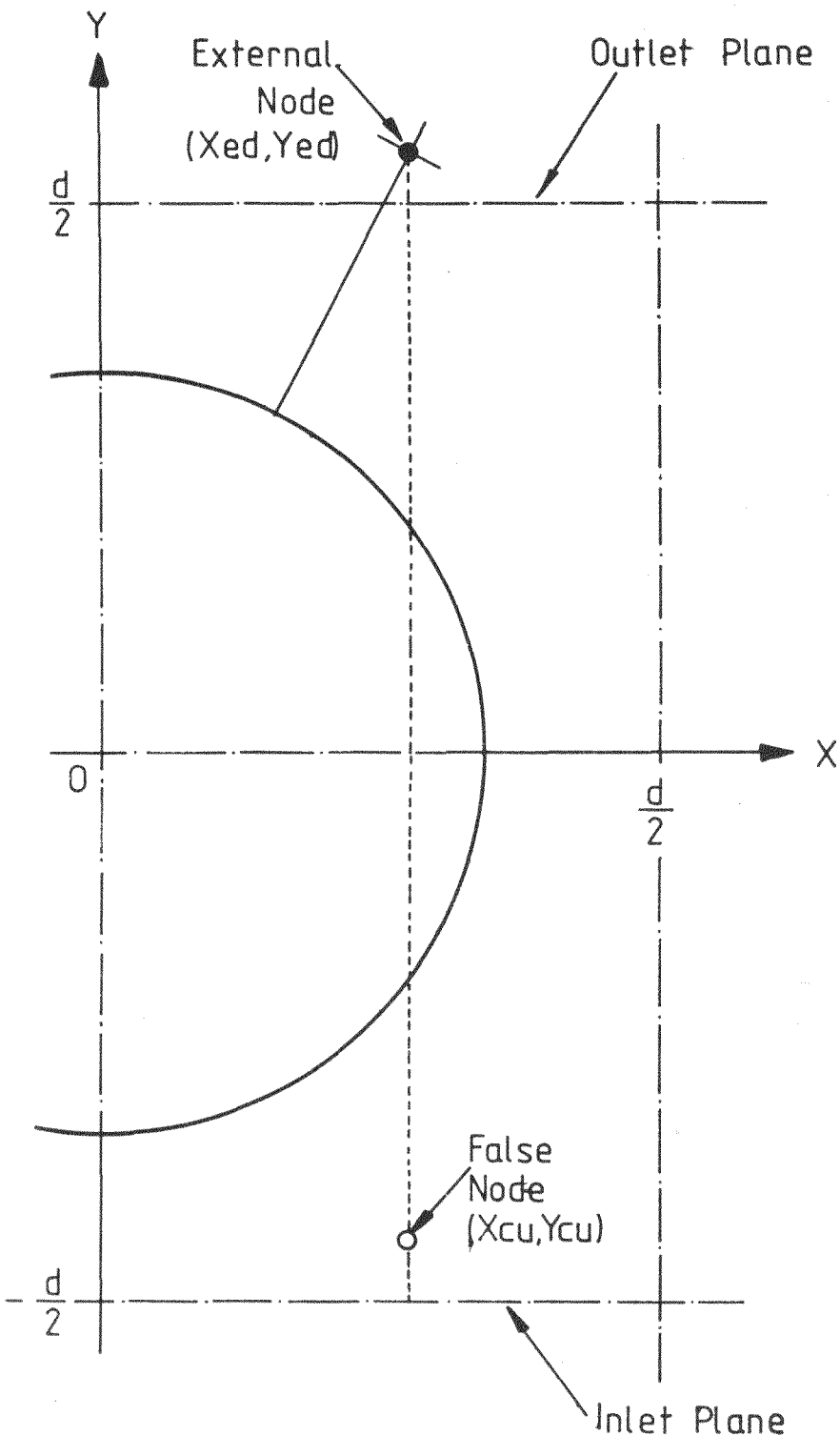

Figure 6 (c) Dowstrem External Node and Corresponding Upstream False Node.

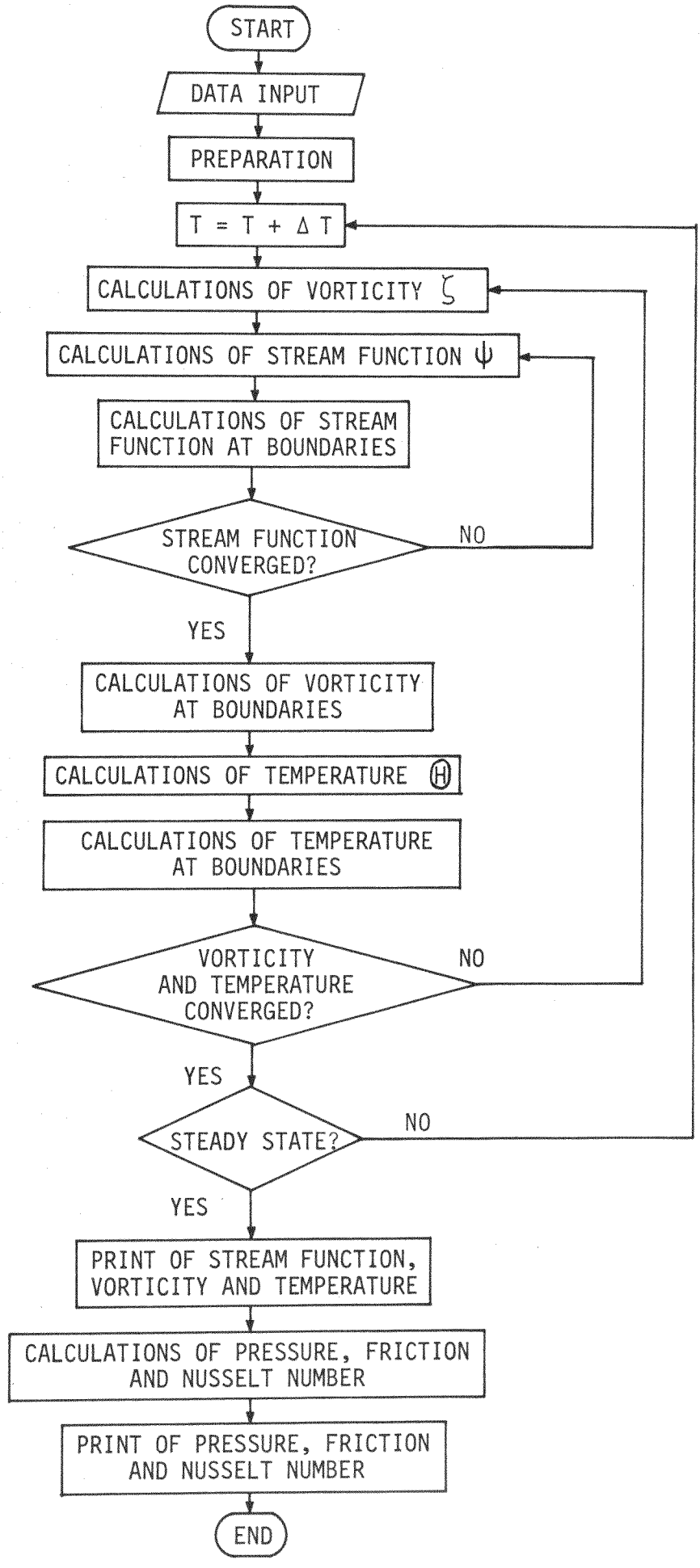

Figure 7. Flow Chart

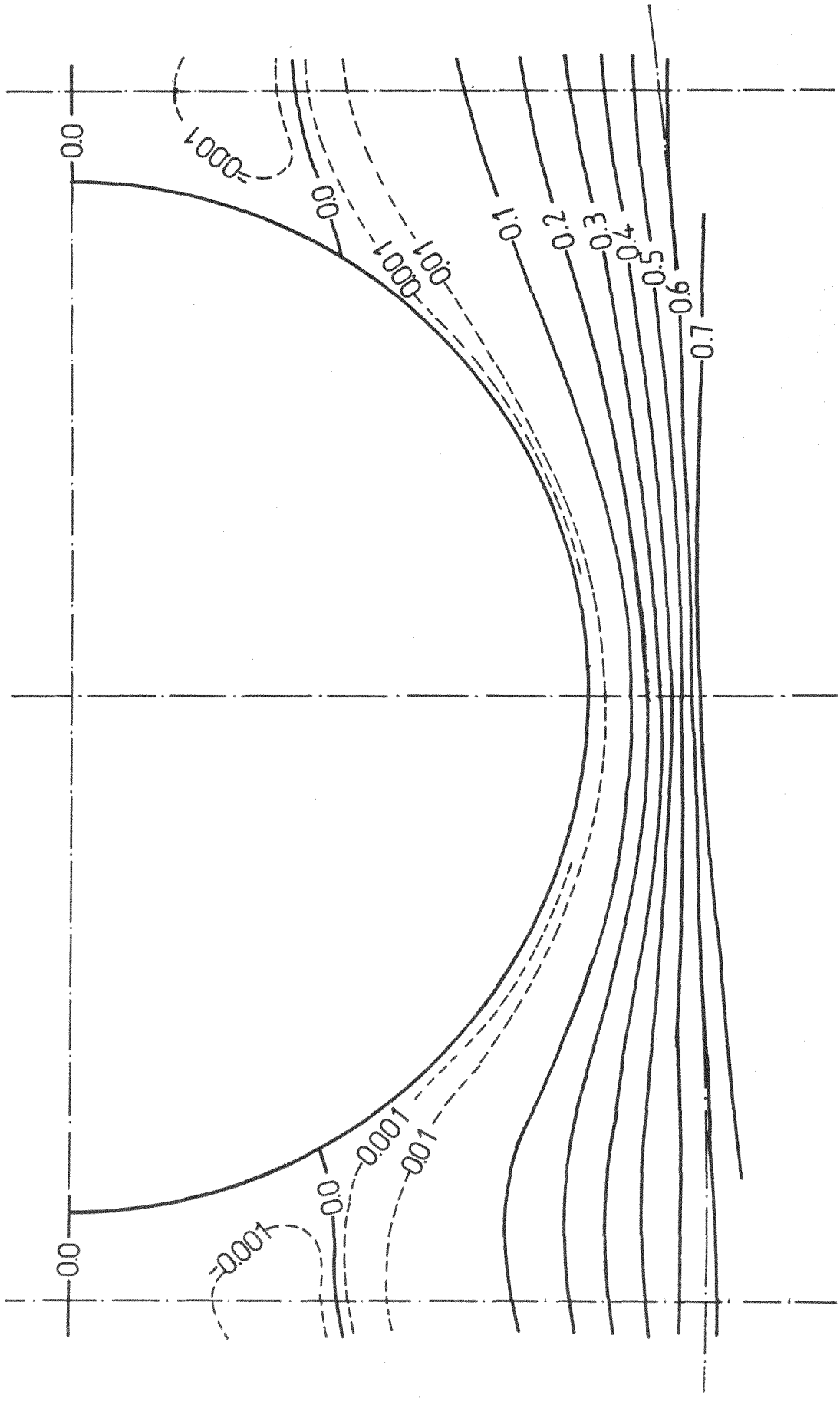

Figure 8 Contours of Stream Function.

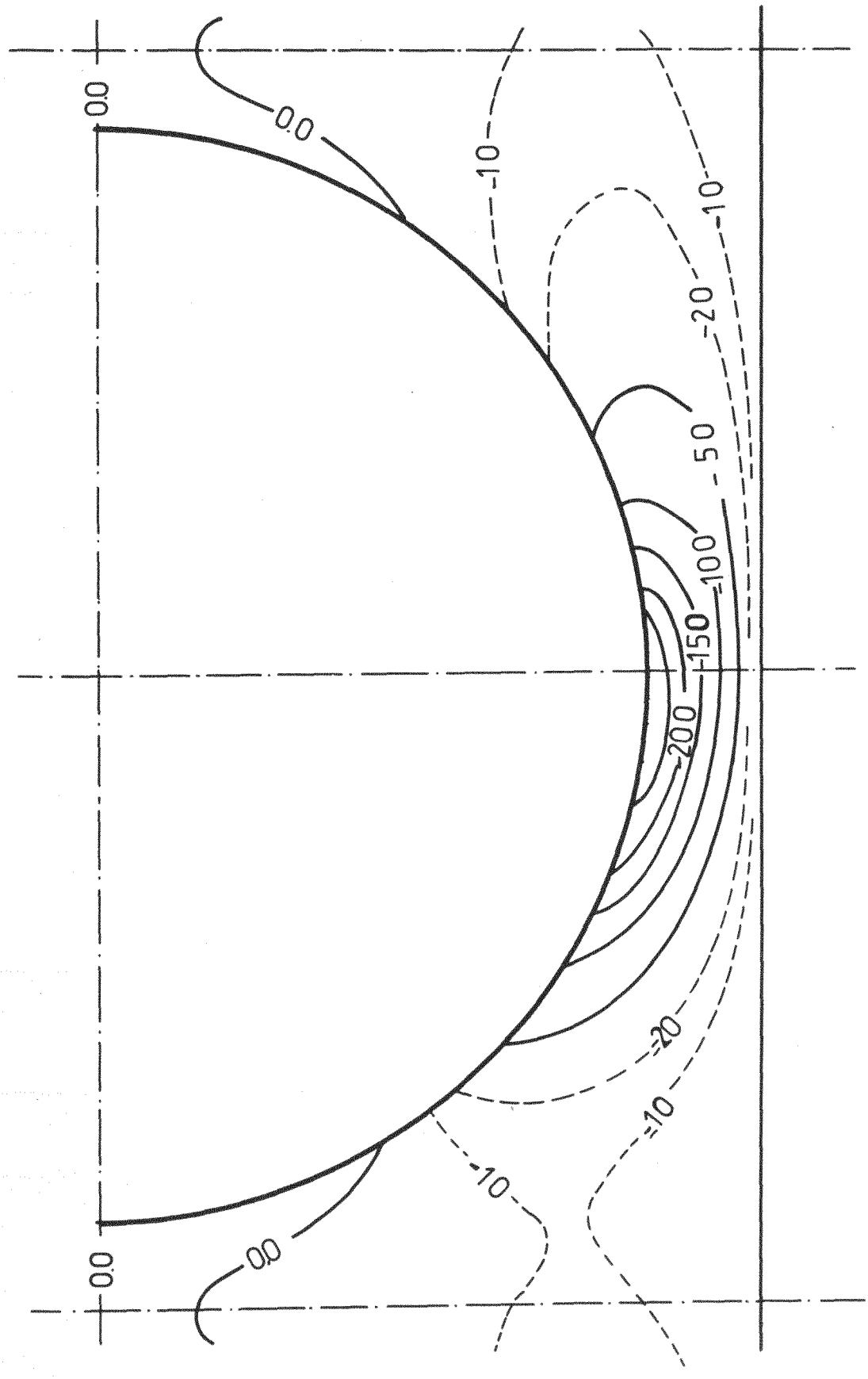

Figure 9. Contours of Vorticity.

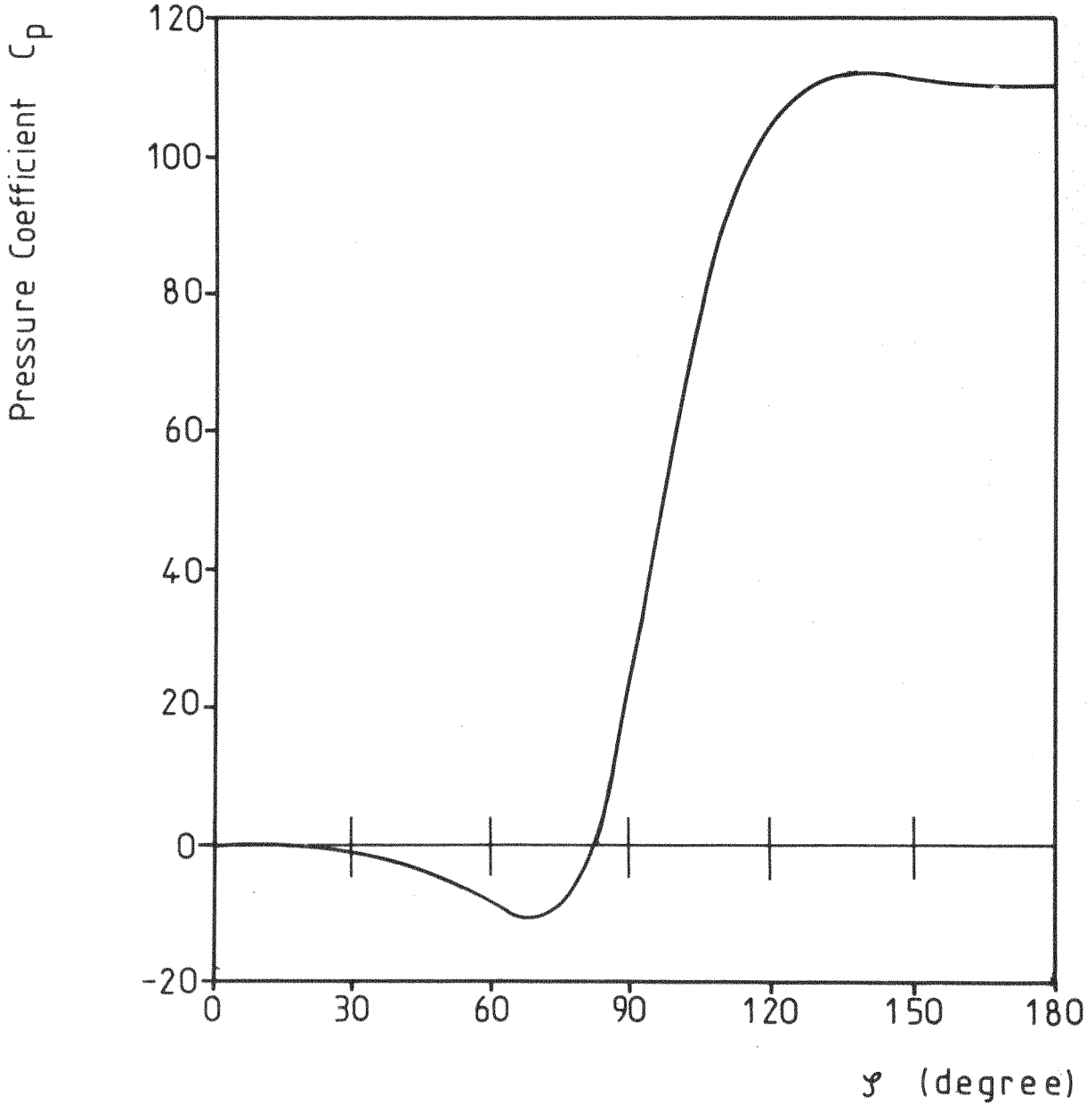

Figure 10. Distribution of Pressure Coefficient

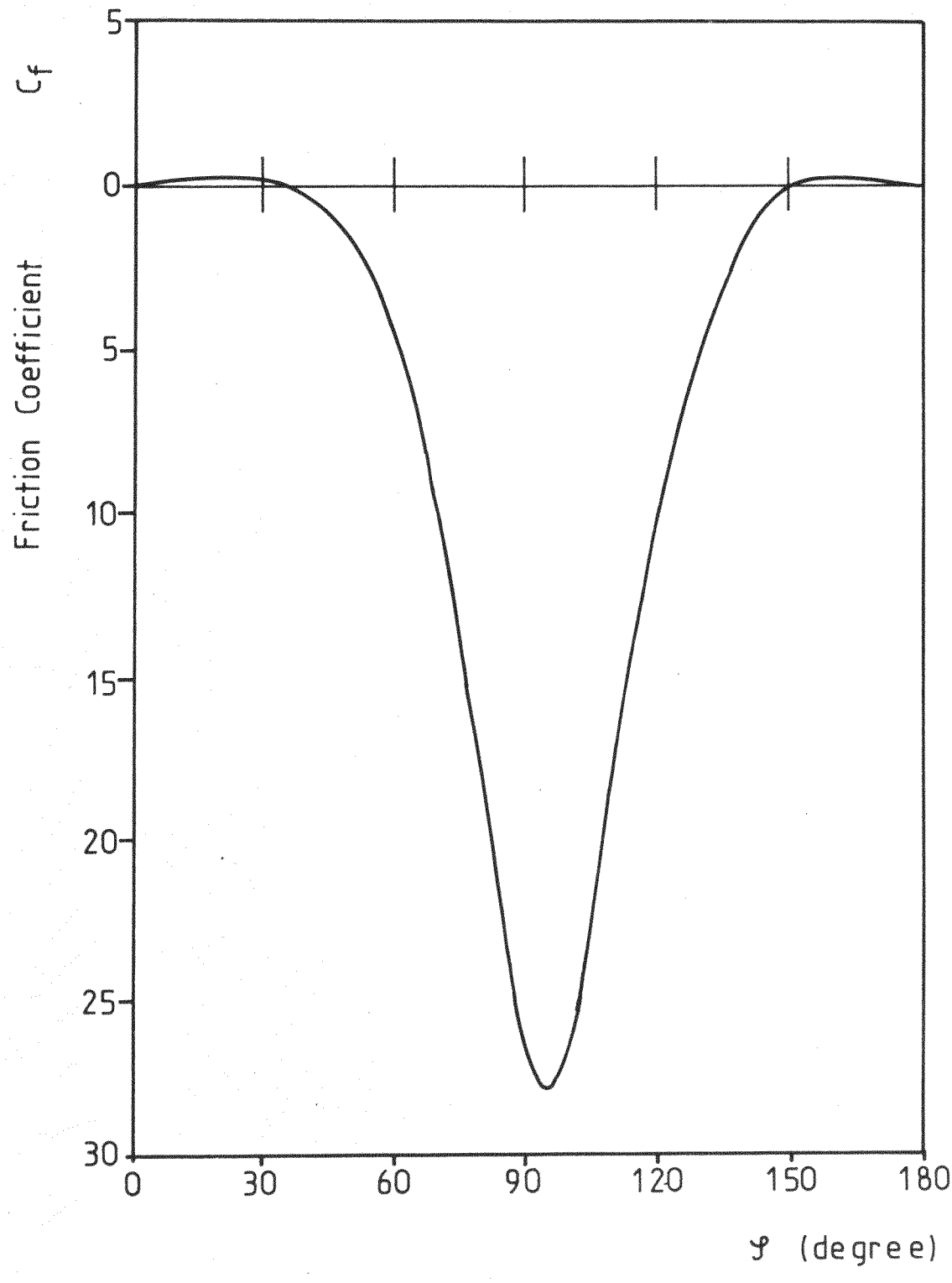

Figure 11. Distribution of Friction Coefficient

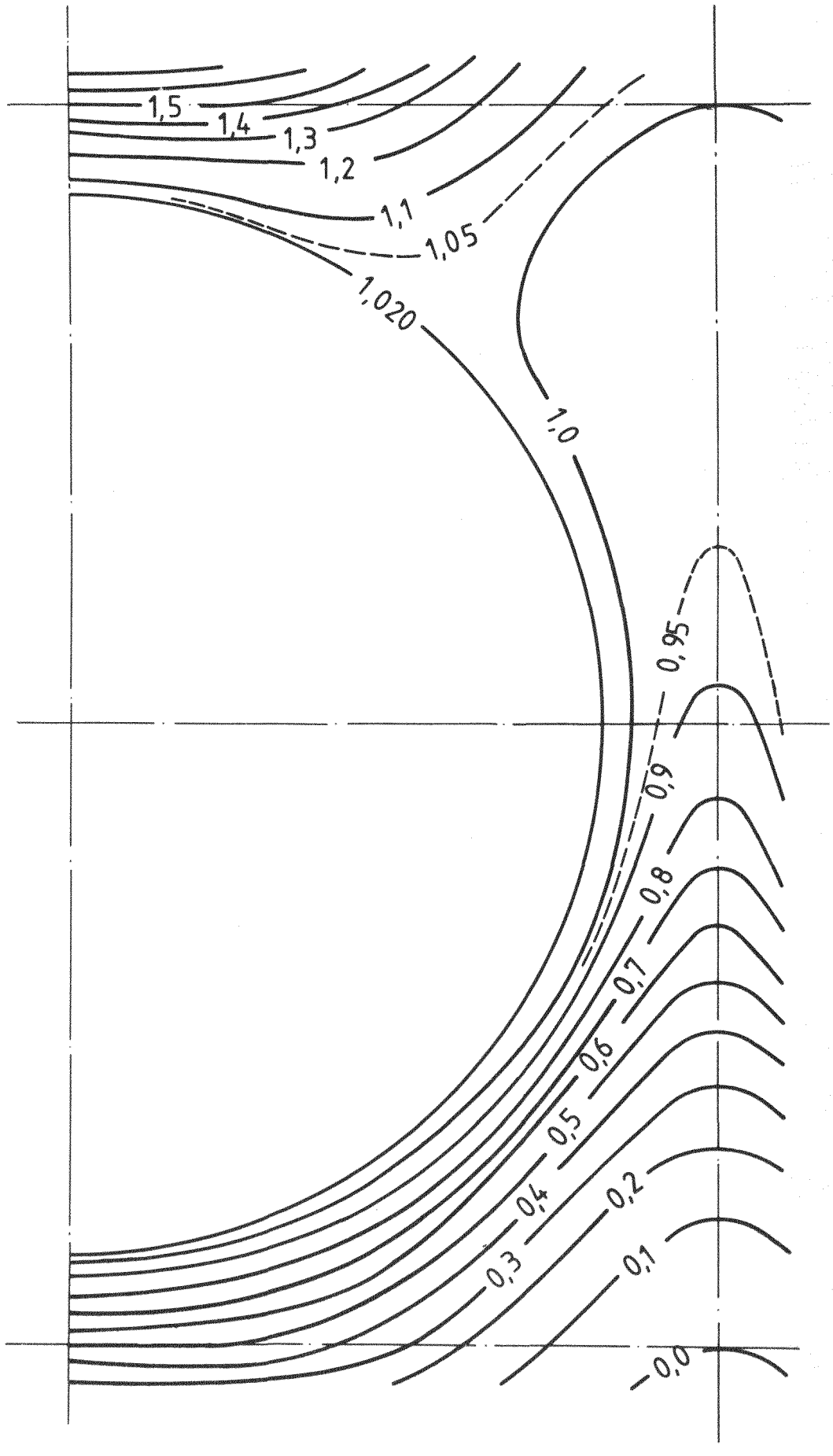

Figure 12. Contours of Temperature

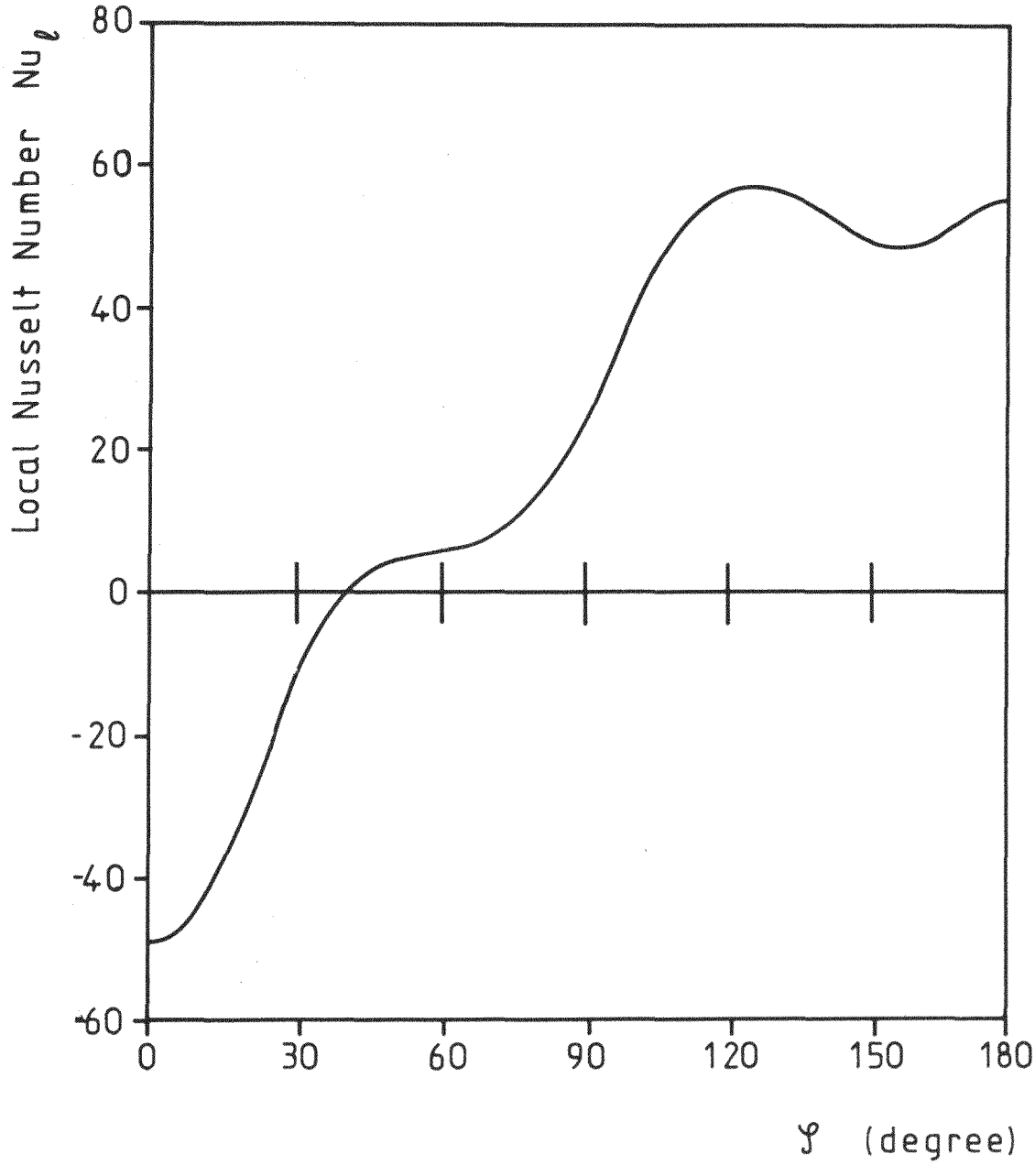

Figure 13. Local Nusselt Number Distribution